Jesús FRAILE-ARDANUY[1], Jesús FRAILE-MORA[1], Pedro A. GARCIA-GUTIERREZ[1]

Technical University of Madrid (1)

Voltage Control of Isolated Self-Excited Induction Generator through Series Compensation

Abstract. *Self-excited induction generators (SEIG) are used in isolated areas to generate electrical energy. In spite of their advantages (low cost, ease of maintenance, etc.) they have poor voltage regulation, even at constant rotor speed. Several voltage regulating schemes using an additional series capacitor to provide additional capacitive VAR with load has been proposed in the literature. In this paper the performance of SEIG through series compensation is investigated comparing computed and experimental results for resistive loads.*

Streszczenie. *Samowzbudne generator indukcyjne są stosowane do wytwarzania energii w izolowanych lokalizacjach. Wadą ich jest słaba możliwość kontroli napięcia, nawet przy stałej prędkości wirnika. W artykule zaproponowano nową metodę kontroli wykorzystująca szeregową kompensację mocy. (**Sterowanie napięciem samowzbudnego generatora indukcyjnego przy wykorzystaniu szeregowej kompensacji mocy**)*

Keywords: Self-excited induction generator
Słowa kluczowe: genersator samowzbudny indukcyjny, kontrola napięcia..

Introduction

Recent developments on distributed power generation have increased the research on suitable generating systems for remote areas using locally available renewable energy sources such as small hydro and wind. Self-excited induction generators (SEIGs) are considered as a viable option due to its specific advantages compared to a conventional synchronous generator [1], among others, one of the key advantages is the inherent over load protection, at the occurrence of a fault. Current will be limited by the excitation, and the machine voltage will collapse immediately. SEIG builds its voltage from residual magnetism, with the help an a.c. capacitor bank that provides the required reactive power from the induction machine. These capacitors are connected in parallel with the SEIG. References [2, 3] present an exhaustive survey about this theme. Anyway, the fundamental problem with SEIGs is its inability to control the terminal voltage and frequency under non-constant load and speed conditions. To regulate the voltage of a SEIG with changing load and speed, self-excitation capacitors may be supplemented with an active external source of reactive power. The function of the voltage regulator is to maintain the output voltage of the generator within a given operating range.

Different methods have been proposed in the literature for regulating the voltage of the SEIGs [4]. The scheme based on switched capacitors [5] finds limited application because it regulates the terminal voltage in discrete steps and it may create switching transients. Also a shunt-connected saturable core reactor may be used as a variable VAR generator. The static VAR compensators (SVC) use a capacitor and inductor with fast switches (GTO´s, thyristors or IGBT´s). Most recent methods are mainly based on either voltage-or-current static capacitors STATCOMs [6, 7] that are based on a DC/AC converter (or inverter), which is able to generate leading o lagging reactive power. These last two methods are often found to be complex with reduced reliability as electronic circuits used therein are prone to failure in field application, and the switching injects harmonics in the line current of the system. Use of additional passive elements to provide self-regulating features therefore was considered worthy of exploration [8-10]. Inclusion of series capacitors to provide additional reactive power with loading is one of the attractive options to improve the regulation of SEIGs. Bim, Szajner and Burian [9] have demonstrated this capability of providing almost flat voltage profile experimentally. Chan [10] has also demonstrated that the long-shunt compensation can be employed to maintain load voltage under various load currents.

While the analysis of SEIG with only shunt capacitors (excitation capacitors) has been well documented [2-3], it is necessary to develop suitable analytical methods to predict the performance of SEIG with series capacitors to facilitate the design of this stand-alone generating unit. In this paper, the voltage control of isolated self-excited induction generator through series compensation is studied. Based on a normalized equivalent circuit model, an analytical method to predict the performance of SEIG in two different cases is developed: 1) output voltage with self-excitation capacitors but without series capacitors and 2) voltage regulation with self-excitation capacitors and including series capacitors. The analytical results are compared with experimental results for resistive loads, verifying the performance of the control method with series capacitors.

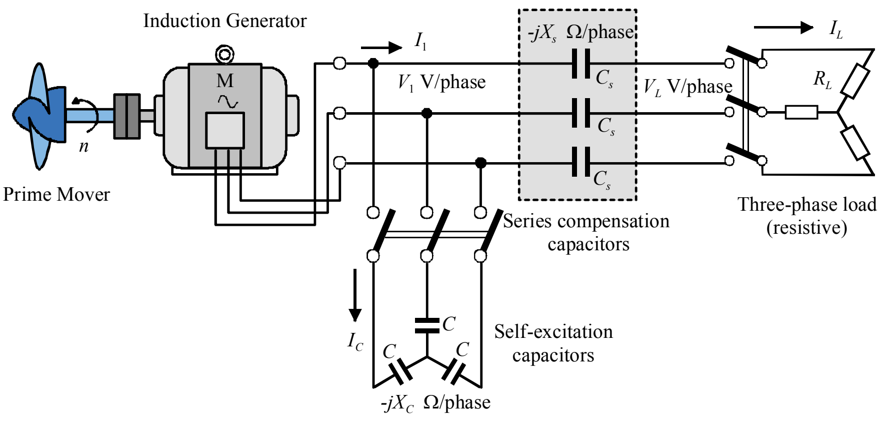

Fig.1. Schematic of the self-excited induction generator with series compensation

Modelling a self-excited induction generator with series compensation

Fig. 1 shows the basic scheme of an SEIG, consists of an induction machine driven by a prime mover which can be a mini hydro turbine or a wind turbine, having three-phase shunt and series capacitors (to provide self-excitation and self–regulation respectively) and a variable three-phase resistance load. The basis of system design is, firstly, to determine the value of shunt capacitors to produce the self-excitation of the generator and, secondly, to calculate the value of series capacitors to ensure that the voltage and frequency of the induction generator are within the desired range. In mini hydro-turbines, the speed can be maintained fairly constant and the voltage regulator (series capacitors) has to maintain the terminal voltage constant at varying loads since frequency drop with load is found to be insignificant. Any voltage regulating scheme has to increase in capacitive VAR with load. The series capacitors achieve this goal under certain conditions, since additional VARs are added as load current increases.

The steady-state equivalent circuit from the scheme of Fig. 1, for any given self-excited frequency f_e is shown in Fig. 2 in which base-frequency values of reactances are retained while the stator and rotor resistances and capacitive reactances are suitable modified. The parameters R_1, R'_2, X_1, X'_2, X_μ, X_C and X_S all referred to the rated o base-frequency f_1 by using a factor $a=f_e/f_1$ (a is the per-unit electric frequency). If the shaft speed is expressed as the factor b of rated o base-synchronous speed (b is the per-unit rotor speed), then slip is defined by $s=(a-b)/a$. In this circuit, only the magnetizing reactance is assumed to be affected by magnetic saturation, and all other parameters are assumed to be constant. In addition, core losses and the effect of the harmonics are ignored.

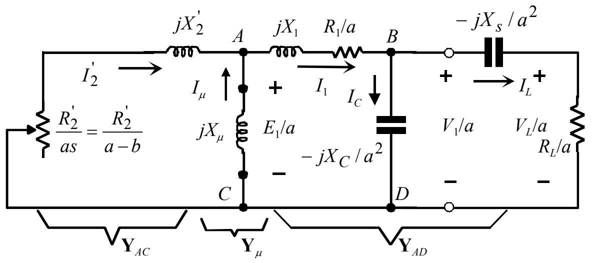

Fig.2. Steady-state equivalent circuit of the SEIG with series compensation and resistive load

The steady-state analysis of the SEIG involves solution of the following problem: given the machine parameters, speed, excitation capacitance, series capacitance and load resistance, it is necessary to determine the value of per-unit electric frequency a and the magnetizing reactance X_μ which enable the balance of active and reactive power across the air gap to be satisfied. Two different solution methods have been proposed, namely, the loop impedance method as used by Murthy et. al. [12] and the nodal admittance method as proposed by Ouazene et. al. [13]. Applying this latest nodal admittance method to the circuit from Fig. 2, the total current at node A may be given by:

$$\frac{\mathbf{E}_1}{a}\left(\mathbf{Y}_{AC}+\mathbf{Y}_\mu+\mathbf{Y}_{AD}\right)=0 \tag{1}$$

Therefore, under steady-state self-excitation, the total admittance must be zero, since $\mathbf{E}_1\neq 0$.

$$\mathbf{Y}_{AC}+\mathbf{Y}_\mu+\mathbf{Y}_{AD}=0 \tag{2}$$

where:

$$\mathbf{Y}_{AC}=\frac{\frac{R'_2}{a-b}-jX'_2}{\left(\frac{R'_2}{a-b}\right)^2+X'^2_2}\ ;\ \mathbf{Y}_\mu=\frac{1}{jX_\mu}=-j\frac{1}{X_\mu} \tag{3}$$

and the admittance $\mathbf{Y}_{AD}$ is:

$$\mathbf{Y}_{AD}=\frac{1}{\mathbf{Z}_{AB}+\mathbf{Z}_{BD}}=\frac{\left(\frac{R_1}{a}+R_t\right)-j\left(X_1-X_t\right)}{\left(\frac{R_1}{a}+R_t\right)^2+\left(X_1-X_t\right)^2} \tag{4}$$

where R_t and X_t are:

$$R_t=\frac{R_L X_C^2}{a(a^2R_L^2+X_C^2)}\quad X_t=\frac{a^2R_L^2X_C+X_sX_CX_T}{a^2(a^2R_L^2+X_T^2)} \tag{5}$$

and condition (2), related to the total admittance, is rewritten as:

$$\frac{\frac{R'_2}{a-b}-jX'_2}{\left(\frac{R'_2}{a-b}\right)^2+X'^2_2}-j\frac{1}{X_\mu}+\frac{\left(\frac{R_1}{a}+R_t\right)-j\left(X_1-X_t\right)}{\left(\frac{R_1}{a}+R_t\right)^2+\left(X_1-X_t\right)^2}=0 \tag{6}$$

Equating to zero the real and imaginary parts in (6), the following two equations are obtained:

$$\frac{\frac{R'_2}{a-b}}{\left(\frac{R'_2}{a-b}\right)^2+X'^2_2}+\frac{\left(\frac{R_1}{a}+R_t\right)}{\left(\frac{R_1}{a}+R_t\right)^2+\left(X_1-X_t\right)^2}=0 \tag{7}$$

$$\frac{X'_2}{\left(\frac{R'_2}{a-b}\right)^2+X'^2_2}+\frac{1}{X_\mu}+\frac{\left(X_1-X_t\right)}{\left(\frac{R_1}{a}+R_t\right)^2+\left(X_1-X_t\right)^2}=0 \tag{8}$$

Equation (7) when multiplied by E_1^2, is related to the conservation principle of the real power, and equation (8) when multiplied by E_1^2, corresponds to conservation of the reactive power. For a given rotor speed, load impedance and excitation and series capacitances, equation (7) is a nonlinear equation in the variable a. After some algebraic manipulations this equation can be expressed as a 7[th]-degree polynomial in a:

$$A_7a^7+A_6a^6+A_5a^5+A_4a^4+A_3a^3+A_2a^2+A_1a+A_0=0 \tag{9}$$

where the expressions of the coefficients A_0 to A_7 (previously normalized by dividing each by $R_L^2\,X_C^2$) can be found in [14].

Solving this equation, real and complex roots are obtained, but only the real ones have a physical significance. Having calculated the value of the variable a, the reactance X_μ can be evaluated using equation (8). For this purpose, this equation is rewritten as follow:

$$X_\mu=\frac{\left(\frac{R_1+aR_t}{a}\right)\left[\left(\frac{R'_2}{a-b}\right)^2+X'^2_2\right]}{\left(X_1-X_t\right)\frac{R'_2}{a-b}-X'_2\left(\frac{R_1}{a}+R_t\right)} \tag{10}$$

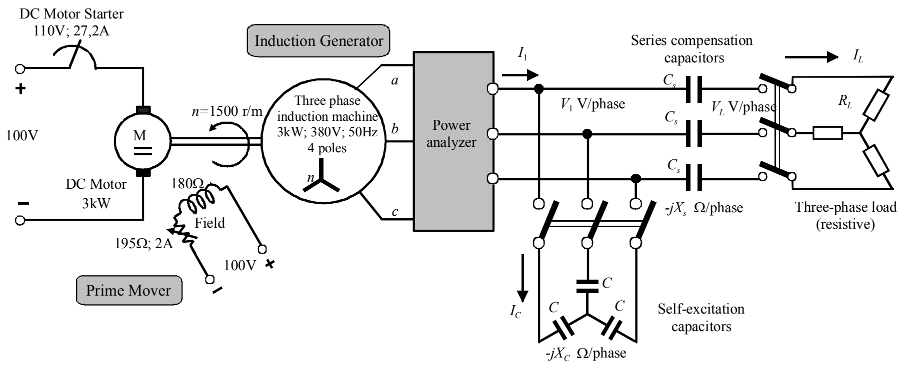

Fig.3. Scheme of the experimental setup

If X_μ is less than the unsaturated value, an operating point exists and the corresponding air-gap e.m.f. E_1 can be read from the magnetization curve (see Fig. 4). The performance characteristics of the generator could be estimated using the following relationships:

A. Stator current

(11) $$\mathbf{I}_1 = \frac{E_1}{a}\cdot \mathbf{Y}_{AD} = \frac{E_1/a}{\left(\frac{R_1}{a}+jX_1\right)+R_t+jX_t}$$

B. Rotor and load current

(12) $$\mathbf{I}_2' = \frac{E_1}{a}\cdot \mathbf{Y}_{AC} = \frac{E_1/a}{\frac{R_2'}{a-b}+jX_2'}$$

$$\mathbf{I}_L = \mathbf{I}_1 \frac{-j\frac{X_C}{a^2}}{\frac{R_L}{a}-j\frac{X_s+X_C}{a^2}} = \mathbf{I}_1\frac{-jX_C}{aR_L-jX_T}$$

C. Terminal stator voltage. Input and load power

(13) $$\mathbf{V}_L = R_L\mathbf{I}_L \quad ; \quad \mathbf{V}_1 = \mathbf{I}_L\left(R_1 - j\frac{X_s}{a}\right);$$

$$P_{in} = \frac{3bR_2'}{a-b}\left|\mathbf{I}_2'\right|^2; \quad P_L = 3R_L\left|\mathbf{I}_L\right|^2$$

Experimental scheme and machine details

The scheme of the experimental setup is shown in Fig. 3 where a power analyser is included to measure all the electric variables (voltages, currents, etc.). The induction generator is a three-phase, 4 poles, 50 Hz, 380 V, 6.5 A, 3 kW, star-connected squirrel cage induction machine. This machine was coupled to a separately excited d.c. drive motor to provide different speeds. Two three-phase variable capacitor banks were connected to the machine terminals to obtain: 1) self-excited generator action (shunt connection) and 2) voltage regulation (series connection). A variable three-phase resistance bank was used to load the induction generator.

Machine parameters required in the analysis were determined experimentally using standard techniques. The parameter values obtained were: R_1=2.03 Ω, R'_2=2.3 Ω, X_1=4.15 Ω, X'_2=4.2 Ω, X_μ=79 Ω.

In order to determine the magnetizing reactance at different airgap e.m.f.s. E_1, the induction generator was driven at synchronous speed (parameter b=1) by the d.c. motor. Then a variable voltage at base frequency (parameter a=1) was applied and the input impedance per phase was measured.

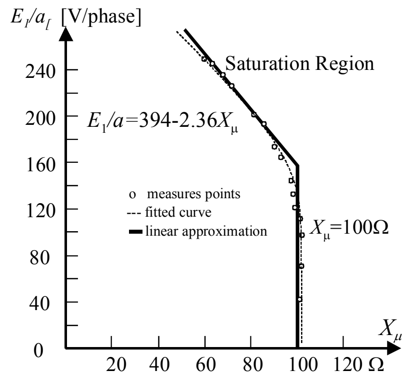

Fig.4. Variation of E_1/a with X_μ

Since the variation of X_μ with the air-gap flux is needed, which is proportional to E_1/a, it is necessary to calculate the airgap e.m.f. by subtracting the voltage drop in the stator impedance from the measured input impedance. X_μ at each voltage is obtained by subtracting the stator impedance from the measured input impedance. Fig. 4 shows the experimental results relating E_1/a, with X_μ for the induction generator of 3kW. Since it is necessary to know the value of E_1/a for a particular X_μ, then X_μ for has been taken as the independent variable. The variation of E_1/a with X_μ will be nonlinear due the magnetic saturation. To simplify the analysis, the variation under saturated region was linearized using the approximate curve drawn in Fig. 4. The function can be expressed by the following equation:

(14) $$E_1/a = 394 - 2.36X_\mu \, ; \, X_\mu = 100\Omega \text{ (unsaturated)}$$

Simulation and experimental results

A. Load characteristics without series capacitors

In this first test, the induction generator is driven at a constant speed of 1500 rpm (synchronous speed, parameter b=1) by a separately excited dc motor. In this test, series capacitors (X_s=0) are not included and there are only self-excitation capacitors with the following values: C= 40, 46, 50 and 56 μF per phase. The generator is gradually loaded by decreasing the load resistance. Fig. 5 shows the variation of load voltage versus load current (left) and load power (right).

In this particular case, equation (9) becomes a 5th-degree polynomial because the coefficients A_0 and A_1 are zero. Solving this equation, four complex roots and one real root are obtained. This latter value is selected as variable a and it is substituted in equation (11), obtaining magnetizing reactance X_μ value. Knowing X_μ, E_1/a is evaluated (from Fig. 4) and then, with the help of equations (12), (13) and (14) the generator response (evolution of the generator terminal voltage as a function of load current and load power) is obtained.

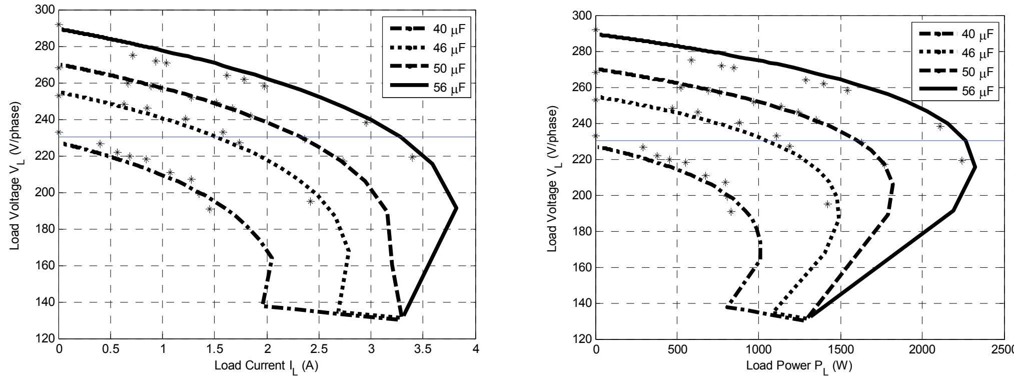

Fig.5. SEIG output voltage with load current and output voltage with load power without series capacitors
"-" Computer Simulation. " * "Test point. n=1500 rpm, C= 40, 46, 50 and 56 μF per phase, X_s=0.

Figure 5 shows that, if the induction generator operates with self-excitation capacitors exclusively, voltage drops are very high and the obtained load power is very small compared with the rating power of the machine. With C=40μF self-excitation capacitors, rated voltage of 230 V at no-load condition (when load current is zero) is obtained, but with higher values of capacitance, no-load voltages are too high, which would be dangerous for the insulation of the generator. A very good agreement can be noticed between the computed and the measured values, which confirms the validity of the equivalent circuit model and the accuracy of proposed solution technique.

B. *Load characteristics with series capacitors*

SEIG with only self-excitation capacitors has a very poor voltage regulation as observed from Fig. 5. For a given self-excitation capacitance, load voltage decreases rapidly with the increase of load current and the generated power is much lower than rated power. By including series capacitors voltage drops are reduced and generated power is increased. This is due to when the load current increases, the current passing through the series capacitors also increases, and more magnetizing reactive power is supplied to the induction generator, and hence voltage drop with load will be less severe compared with that obtained in the simple SEIG.

Again, the induction generator is driven at a constant speed of 1500 rpm (parameter b=1) by a separately excited dc motor. In this test only a self-excitation capacitance (C=40 μF) is used because with this value, a rated voltage of 230 V at no-load condition is obtained, as it is shown in Fig. 5. Then, three values of series capacitances: C_S=50μF, C_S=100 μF and C_S=150 μF are evaluated. For each value of series capacitance, the generator is gradually loaded by decreasing the load resistance. The main characteristics of this SEIG with series capacitors are shown in Figures 6 and 7. It is shown in Fig. 6 (top) the variation of load voltage versus load current and the generator voltage (terminal voltage) versus load current (bottom). Fig. 7 shows the variation of load voltage with load power.

In this case, equation (9) becomes a 7^{th}-degree polynomial and solving this equation, six complex and one real roots are obtained. Substituting this latter value for the variable a in the equation (11), the value of the magnetizing reactance X_μ is obtained and finally, the generator response is calculated.

The experimental values are very close to the corresponding simulation results (as shown in Fig. 6 and 7). In Fig. 6, voltage curves for capacitors C_S=100 μF and C_S=150 μF, are very similar, corresponding to capacitances of the order of 2.5-4 times the self-excitation capacitance. Both responses provide smaller voltage variations than for capacitance value of C_S=50μF. However, it is shown that the generator terminal voltage V_1 (shown at the bottom of the Fig. 6), for high load currents, is higher when the capacitance values are C_S=50 or 100 μF, and it can produce the magnetic saturation of induction generator. Therefore the best solution for this laboratory machine implementation is to choose the series capacitor value of C_S=150 μF. Fig. 7 shows load voltage versus load power: for C_S=50 μF the load power is limited to 2000W, however with the capacitances values of C_S=100 μF and C_S=150 μF, the machine can deliver its rated power almost without voltage drop. Therefore the inclusion of series capacitance results in the higher overload capability of the machine.

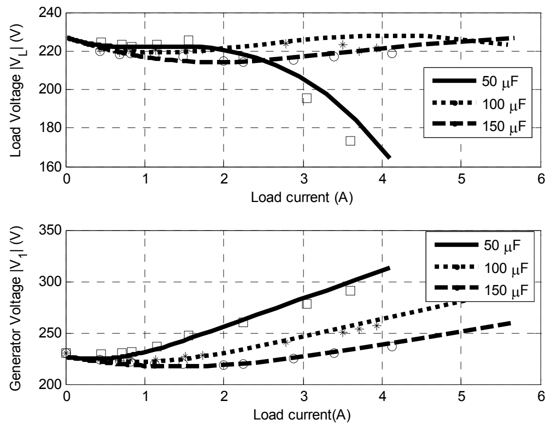

Fig.6. SEIG output voltage and load voltage versus load current with series capacitors.
"-" Computer Simulation. " * " Test point. n=1500 rpm, C= 40μF per phase, C_s= 50-100-150μF.

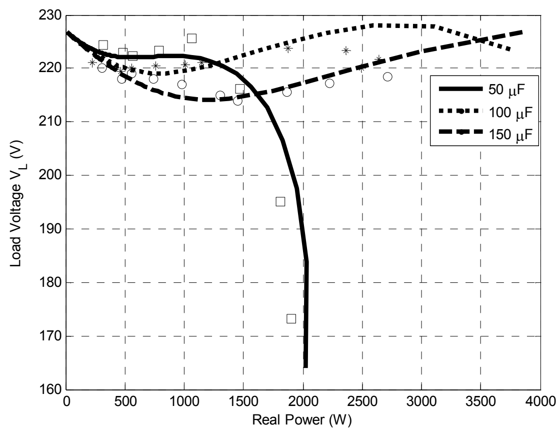

Fig.7. SEIG output voltage versus load power with series capacitors
"- " Computer Simulation. " * " Test point. n=1500 rpm, C= 40μF per phase, C_s= 50-100-150μF.

Conclusions

This paper presents a simple analytical method based on nodal admittance to obtain the steady state characteristics of an isolated self-excited induction generator, namely, the simple SEIG, which has only self-excitation capacitors, and SEIG with series compensation. The method leads to two simultaneous equations which can be solved to obtain saturated magnetizing reactances at p.u. generated frequency (variable a) for the given machine parameters, load resistances, speed, and capacitors (both self-excitation o shunt and series). It is demonstrated that the voltage regulation and power capability of the SEIG are both remarkably improved with a proper choice of self-excitation capacitance and series capacitance. Experimental results obtained on a 3kW laboratory machine confirm the validity and accuracy of the proposed method.

Acknowledgments

This work has been developed within the framework of the activities of the Project: "Development of a turbo-generator for electric power generation in artificial recharge of aquifers" and has been carried out for the Energy Research Center located in Totana (Murcia), Spain (University-Industry Research). The authors wish to place on record its deep sense of gratitude to D. Jose Maria Pérez, CEO of Perga Engineers, for their valuable assistance in this project.

REFERENCES

[1] M. G. Simoes, M.G, F. A. Farret, *Renewable Energy Systems, Design and Analysis with Induction Generator*, (2002), CRS Press, Boca Raton, Fl.

[2] G. K. Singh, Self-Excited Induction Generator Research - A Survey, *Electric Power Systems Research*, 69 (2004), 111-114.

[3] R. C. Bansai, Three-Phase Self-Excited Induction Generators: An Overview, *IEEE Trans. on Energy Conversion*, 20 (2005), No 2, 292-299.

[4] Y. K. Chauhan, S. J. Jain, B. Singh, A Prospective on Voltage Regulation of Self-Excited Induction Generator for Industry Applications. *IEEE Trans. on Industry Applications*, 46 (2010), No 2, 720-730.

[5] Singh, S.P; Singh, Bhim; Jain, M.P, Performance Characteristics and Optimal Utilization of a Cage Machine as Capacitor Excited Induction Generator. *IEEE Trans. on Energy Conversion*, 5 (1990), No 4, 679-685.

[6] Singh, Bhim; Shilpakar, L.B, Analysis of a Novel Solid State Voltage Regulator for a Self-Excited Induction Generator. *IEE Proceedings Generation, Transmission and Distribution*, 145 (1998), No. 6, 647-655.

[7] Singh, Bhim; Murthy, S.S, Gupta, S, A Voltage and Frequency Controller for Self-Excited Induction Generators. *Electric Power Components and Systems*, 34 (2006), 141-157.

[8] Chan, T.F, Steady-State Analysis of Self-Excited Induction Generators, *IEEE Trans. on Energy Conversion*, 9 (1994), No 2, 288-296.

[9] Bim, E; Szajner, J; Burian, Y, Voltage Compensation of an Induction Generator with Long-Shunt Connection. *IEEE Trans. on Energy Conversion*, 4 (1989), No 3, 536-530.

[10] Chan T.F, Analysis of Self-Excited Induction Generators using an Interative Method, *IEEE Trans. on Energy Conversion*, 10 (1995), No 3, 502-507.

[11] Wang, L; Su, J, Effects of Long-Shunt and Short-Shunt Connections on Voltage Variations of a Self-Excited Induction Generator, *IEEE Trans. on Energy Conversion*, 12 (1997), No 4, 368-374.

[12] Murthy, S.S; Malik, O.P; Tandon, A.K, Analysis of Self-Excited Induction Generators, *IEE Proceedings of IEE*, 129 (1982), Pt. C, No 6, 260-265.

[13] Ouazene, L; McPherson, G, Analysis of the Isolated Induction Generator, *IEEE Trans. on Power Apparatus and Systems*, 12, PAS-102 (1983), No 8, 2793-2798.

[14] Fraile-Ardanuy, J.; J. Fraile-Mora and P. García-Gutiérrez, Voltage Control of Isolated Self-Excited Induction Generator through Series Compensation, *Proc. Of the 12th Portuguese-Spanish Conference in Electrical Engineering,* Azores (2011).

***Authors**: J. Fraile-Ardanuy, Departamento de Tecnologías Especiales Aplicadas a la Telecomunicación, ETS Ingenieros de Telecomunicación. Technical University of Madrid. Avda. Complutense, 30. Ciudad Universitaria, 28040 Madrid (Spain). Phone number: +34 91 549 57 00. Ext. 2328, e-mail address: jfraile@etsit.upm.es J. Fraile Mora and P. García-Gutiérrez. Departamento de Ingeniería Civil: Hidráulica y Energética. ETS Ingenieros de Caminos, Canales y Puertos. Technical University of Madrid. c/ Profesor Aranguren s/n, 28040 Madrid (Spain) frailemora@caminos.upm.es, pgar@caminos.upm.es.*